JOURNAL OF MATERIALS SCIENCE 21 (1986) 717–724

Crack branching and arrest in environmental cracking of polyethylene

J. L. BELCHER*, H. R. BROWN‡
Department of Materials Engineering, Monash University, Clayton, Victoria 3149, Australia

At intermediate K values a region where the crack speed is constant, that is, independent of K, is observed in detergent cracking of low density polyethylene. This region is terminated at high K by one of two processes: in thin specimens the crack arrests, and in thick specimens it branches. The mechanism of crack branching involves the crack front twisting and then the initiation of a new crack at the centre of the specimen. A model has been proposed to explain this mechanism and also the fact that crack arrest or branching occur at approximately the same K value. After branching the cracks continue to propagate at constant speed along paths where $K_{II} \approx 0$ and if the specimen is wide enough, can branch again.

1. Introduction

Three separate modes of failure have been shown to exist in environmental stress cracking (ESC) of low density polyethylene. Any one material/environment combination can probably show any of the three modes depending on the driving force for crack propagation and the physical properties (such as viscosity) of the fluid. This has been demonstrated by Shanahan and Schultz [1] in a series of constant stress, time to fail experiments on unnotched polyethylene specimens immersed in silicone oils and also by Bandyopadhyay and Brown [2] in crack propagation experiments on polyethylene immersed in detergents. The three modes are believed to be: (I) relaxation controlled growth at low stress, (II) fluid flow controlled growth at intermediate stresses, and (III) failure similar to that seen in the absence of the environment at high stresses. Low density polyethylene (LDPE) is a very ductile material in air so mode (III) failure is essentially ductile. The brittle cracks observed in modes (I) and (II) cease propagation at transition to mode (III).

As the transition from modes (II) to (III) is from brittle to ductile failure it seems likely that it might be related to a plane strain to plane stress transition and hence depend on the thickness of the specimen. The aim of the current work was to examine this hypothesis by increasing the specimen thickness from the value of about 1 mm used previously. Thickness was indeed found to be important; and when the specimen was thicker than 2.5 mm, the mode (III) failure was never observed. Instead, the crack branched and the two cracks propagated in a brittle manner and in some cases branched again.

It is not surprising that crack branching occurs in this system. Crack branching has previously been observed to occur during the similar phenomenon of stress corrosion cracking of various metals [3–7]. Experimental observations have indicated that attainment of a region of constant crack speed, independent of stress intensity factor, is necessary if crack branching is to occur during the stress corrosion cracking of a particular metal/environmental pair. Such a region of constant crack speed is observed during the ESC of polyethylene in the detergent solution environment used in this work. Hence the occurrence of crack branching was quite likely.

From simple energy considerations it is obvious that if the constant crack speed region (mode II) occurs over a range of K_I of a factor of $2^{1/2}$, then there is sufficient energy available to drive two cracks instead of one. This can be considered as a necessary condition for cracking branching but is not sufficient; a mechanism for the formation of the second crack is still required. The actual process of crack branching was observed using time lapse photography and from these observations a mechanism for the formation of the brittle crack will be proposed.

2. Material and experimental techniques

The low density polyethylene used for the experiments described in this paper was XJG 143 (density 0.918 g cm^{-3}, melt flow index = 2.5) manufactured by ICI Australia Pty Ltd. From this polymer compression moulded sheets of thickness (B) 1.35, 2.40 and 3.90 mm were made. Single edge-notched (SEN) specimens were cut from these sheets and the notches sharpened with a razor blade. The experiments were conducted in a dead weight load apparatus which incorporated a travelling microscope, with an accuracy of 0.02 mm for monitoring the crack length. Alternatively the crack length was measured to an accuracy of 0.1 mm from negatives taken at fixed intervals by a motor driven camera mounted in a fixed position on the travelling microscope rails. The stress

* *Present address*: Australian Road Research Board, 500 Burwood Highway, Vermont South, Victoria 3133, Australia.
‡ *Present address*: IBM San Jose Research Laboratory, 5600 Cottle Road, San Jose, CA 95193.

0022–2461/86 $03.00 + .12

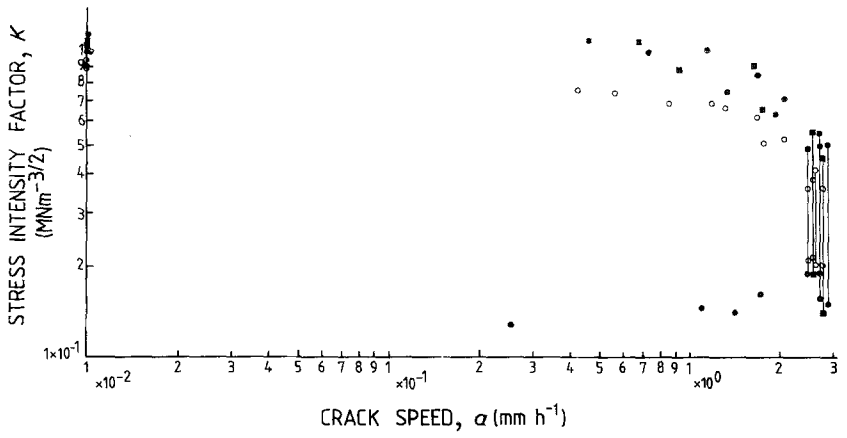

Figure 1 Graph of crack growth behaviour for unsoaked specimens. ● B = 1.35, ■ 2.40 mm, W = 90 mm; ○ B = 1.35 mm, W = 30 mm.

intensity factor, K, was calculated using the equation of Brown and Srawley [8]. The environment used for these experiments was a 10% by volume solution of Igepal Co630.

Specimens 90 mm wide (W = 90) were cut from the 1.35, 2.40 and 3.90 mm thick sheets. Most of these specimens were loaded with 13.5, 24 and 39 kg, respectively, and had initial crack lengths such that the initial stress intensity factors were in the range 0.10 to 0.19 MNm$^{-3/2}$. However different loads were applied to three of the 3.90 mm thick specimens. These will be referred to specifically when relevant.

In addition some ESC specimens 30 mm wide were cut from the 1.35 mm thick sheets. These specimens were subjected to an applied load of 6 kg and had initial stress intensity factors of approximately 0.20 MNm$^{-3/2}$.

The ESC experiments dicussed in this paper were commenced within 12 h of immersion of the unstressed specimen in the detergent solution.

3. Crack deceleration – results and discussion

The crack growth behaviour of the specimens 1.35 and 2.40 mm thick are shown in Fig. 1. For all specimens crack growth at values of K in excess of 1.2 MNm$^{-3/2}$ was very erratic with short bursts of crack growth followed by substantial periods of no growth. This behaviour is not recorded in Fig. 1 and will not be discussed in this paper.

The K–a relationship for the specimens with B = 1.35 mm and W = 90 mm was of the same form as that reported by Bandyopadhyay and Brown [2, 9] who observed regions of accelerating, followed by constant and finally decelerating crack growth with increasing K for various grades of LDPE in Igepal Co630 solution.

For the specimens with B = 2.40 mm and W = 90 mm, no region of accelerating crack growth was observed. This (and the absence of the accelerating crack growth region for the 3.90 mm thick specimens) suggests that this phenomenon may be thickness dependent. The specimens with B = 1.35 mm and W = 30 mm had initial K values greater than those at which the accelerating crack growth region might be observed.

Neither specimen thickness nor specimen width appear to influence the range of constant crack speeds observed. (This region is considered to occur because of restrictions in the ability of the fluid to flow into the craze which is present at the crack tip.) The K value at the onset of crack deceleration also appears to be independent of specimen thickness. However, specimen width appears to have an influence on this value as well as on the value of K at which regular crack growth ceased. For the specimens 30 mm wide, the onset of the decelerating crack growth region and the end of regular crack growth occurred, respectively, at K = 0.36 to 0.41 MNm$^{3/2}$, and at K = 0.89 to 1.0 MNm$^{-3/2}$. For the specimens 90 mm wide, the same events did not occur until K = 0.45 to 0.55 MNm$^{-3/2}$ and K = 1.0 to 1.2 MNm$^{3/2}$, respectively. These results suggest that at these high Ks the crack propagation is not entirely controlled by K. As K is based on linear elasticity and LDPE is by no means a linear material, this is not surprising.

Bandyopadhyay [10], based on observations of the fracture surfaces, attributes the occurrence of crack deceleration to a change in the type of failure from plane strain failure to plane stress failure. A series of photographs typical of the fracture surface of all specimens is shown in Fig. 2. The fibril size is seen to increase gradually throughout crack growth. The change to crack deceleration began in Fig. 2d. No change in crack propagation mode from plane strain to plane stress behaviour is evident on the fracture surface in this region. The onset of crack deceleration did coincide with an observed change in the specimens. This is shown in Fig. 3. From crack length measurements one finds that the region of straight crack path on the left corresponds to the end of the region of constant crack growth. The irregular crack path on the right corresponds to the early stages of decelerating crack growth.

4. Crack branching – results and discussion

The crack growth behaviour of the 3.90 mm thick specimens was characterized by crack branching as shown in Fig. 4. In these specimens no region of accelerating crack growth was observed. In specimens with an initial stress intensity factor less than 0.10 MNm$^{-3/2}$ no detectable crack propagation occurred in 16 h at which stage the experiments were terminated. The maximum speed with which a crack could have propagated undetected was 10^{-3} mm h^{-1}.

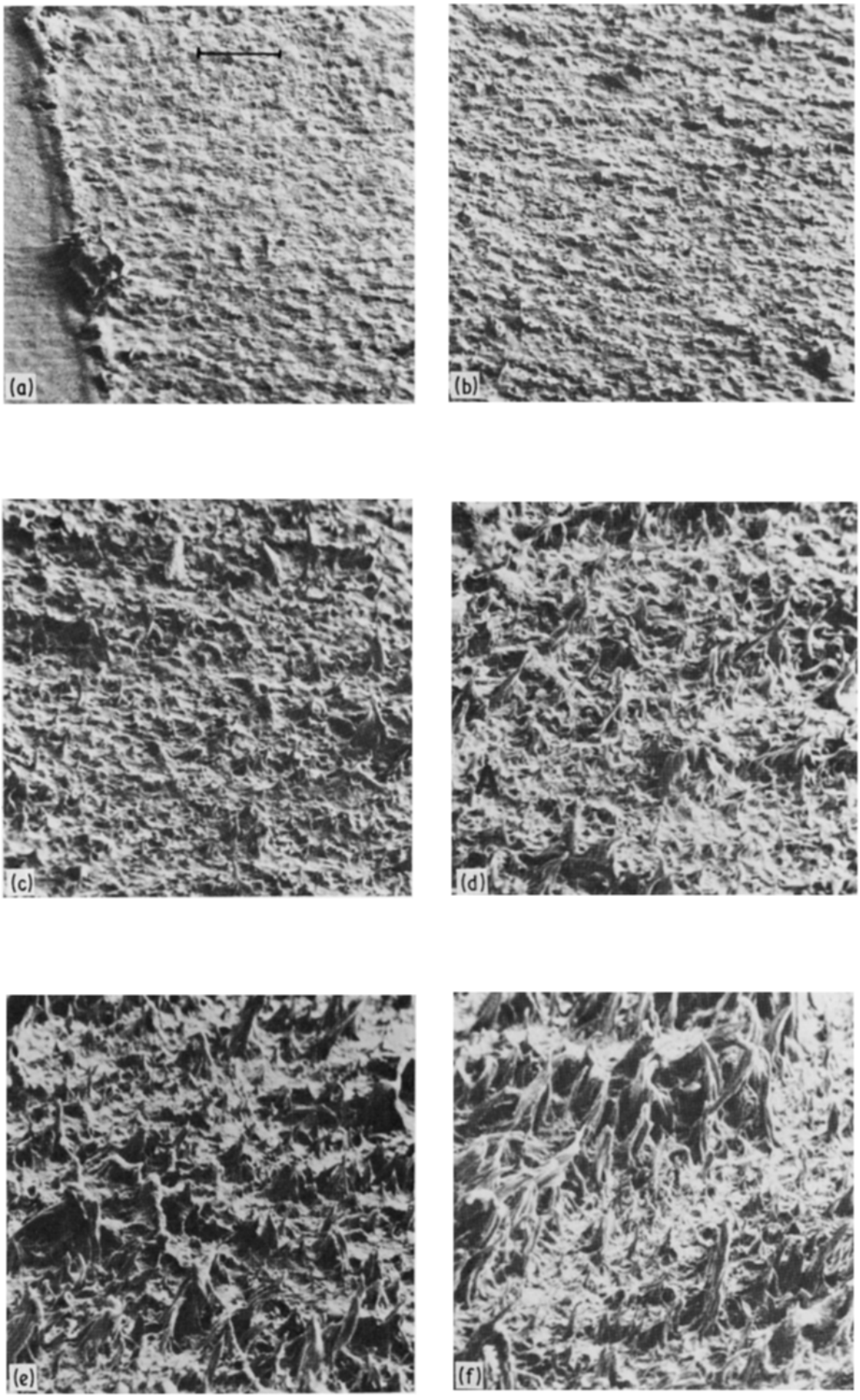

Figure 2 Fracture surface typical of 1.35 and 2.40 mm thick specimens Scale $= 50\,\mu m$ (a) $K = 0.13\,MNm^{-3/2}$, (b) $K = 0.23\,MNm^{3/2}$, (c) $K = 0.32\,MNm^{-3/2}$, (d) $K = 0.49\,MNm^{-3/2}$, (e) $K = 0.61\,MNm^{-3/2}$ and (f) $K = 0.90\,MNm^{-3/2}$.

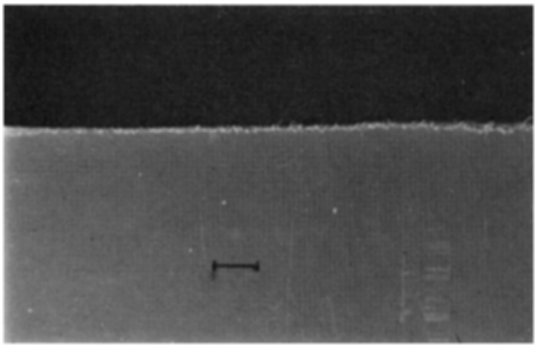

Figure 3 Fracture path typical of 1.35 and 2.4 mm thick specimens. Scale = 1 mm.

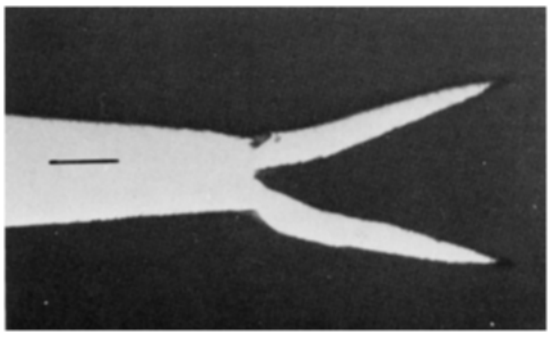

Figure 4 The crack growth behaviour of the 3.90 mm thick SEN specimens was characterized by crack branching. Scale = 20 mm.

For specimens with an initial stress intensity factor equal to or in excess of $1.12\,MNm^{-3/2}$, detectable crack propagation occurred within 0.5 h of loading. The initial crack growth behaviour of these specimens was observed to be that of constant crack speed ($\dot{a}$ = 2.6 to 2.9 mm h^{-1}) with increasing stress intensity factor.

This range of constant crack speeds is very similar to the range observed in the 1.35 and 2.40 mm thick specimens (2.5 to 2.9 mm h^{-1}) which indicates that, as expected, the constant crack speed is independent of specimen thickness. Table I records the loads applied to the 3.90 mm thick specimens and the individual constant crack speeds observed. It also gives information on the crack branching behaviour of the specimens.

It can be seen that all 3.90 mm thick specimens could be classified as one of two types depending on the stress intensity factor at which crack branching occurred. The a/W ratio is obviously not the controlling parameter as in specimens 4, 7 and 8, with applied loads other than the usual 39 kg, crack branching was observed to occur within the same stress intensity factor ranges; although this meant that crack branching occurred at different a/W ratios. For specimens 1, 2, 3 and 4 where crack branching occurred when $K = 0.45 - 0.51\,MNm^{-3/2}$, the crack path was straight up to the beginning of crack branching. These specimens will be referred to as type I specimens. In the remainder of the specimens (type II) the crack path became irregular at (approximately) $K = 0.48$ to $0.50\,MNm^{-3/2}$ (Fig. 5) and crack branching did not occur until $K = 0.68$ to $0.74\,MNm^{-3/2}$.

Thus all 3.90 mm thick specimens underwent a change in crack propagation when $K = 0.45$ to $0.51\,MNm^{-3/2}$. This falls within the range $K = 0.45$ to $0.55\,MNm^{-3/2}$ at which crack deceleration was observed to begin in the 1.35, 2.40 mm thick, 90 mm wide specimens. The irregular fracture path observed to begin within this K range in type II specimens (Fig. 5) is similar to the irregular fracture path observed during crack deceleration in the thinner specimens (Fig. 3), and indeed the crack was observed to decelerate slightly in the type II specimens over this region. The above observations, and the observation that one of the crack branches always initiates in the centre of the specimen, leads to the conclusion that crack branching and crack deceleration are related phenomena.

Fig. 6, shows a sequence of photographs of a crack tip taken during crack branching. The appearance of the crack tip before branching begins is shown in Fig. 6a. The crack front then "twists" and two crack tips, rather than the single planar crack front, are formed. This is shown in Fig. 6b where the two portions of the crack front can be seen. Crack tip A opens onto the surface that shall be termed the "front" of the specimen. Crack tip B opens on to the "back" of the specimen. Fig. 6b was taken at what will be designated time t = 0 min. Fig. 6c and d shows the crack at t = 35 min from the front and the back of the specimen, respectively. In Fig. 6c it can be seen that a third crack tip, C, is present below crack tip A. Fig. 6d shows crack tips B and C only, crack tip A is obscured. C is an internal crack at this stage, being open neither to the front nor the back of the specimen. Fig. 6e and 6f show the crack at t = 70 min again from the front and back of the specimen, respectively. In Fig. 6e it can be seen that crack tips B and C have grown noticeably. Crack tip A is being "overrun" as crack tip B grows through from the back to the front of the specimen. This can be seen more clearly in

TABLE I

Specimen number	Load (kg)	K at onset of irregular fracture path ($MNm^{-3/2}$)	K at crack branching ($MNm^{-3/2}$)	a/W for irregular fracture path	a/W for crack branching	Specimen type
1	39	–	0.45	–	0.26	I
2	39	–	0.46	–	0.27	I
3	39	–	0.51	–	0.29	I
4	24	–	0.48	–	0.40	I
5	39	0.48	0.74	0.28	0.40	II
6	39	0.49	0.68	0.28	0.37	II
7	42	0.50	0.70	0.27	0.36	II
8	48	0.50	0.68	0.23	0.31	II

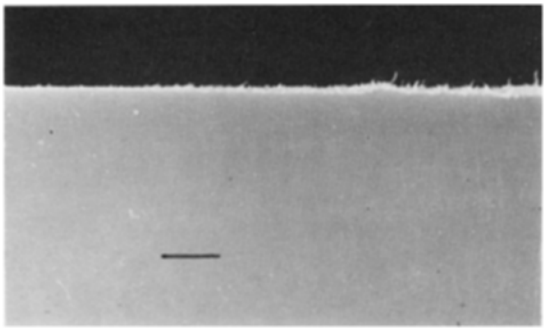

Figure 5 Fracture path typical of 3.90 mm thick type II specimens. On the left the crack path is smooth. The irregular crack path on the right was produced during the region of crack deceleration. Scale = 2 mm.

Fig. 6f where there is only a small portion of material keeping crack tip A independent of B. Crack tip C is still an internal crack. Fig. 6g shows the crack at $t = 120$ min. Crack tips B and C are obviously opening. Crack tip C is no longer internal. The remains of crack tip A can just be seen. In Fig. 6h the well established crack branches B and C are shown at $t = 240$ min. This sequence of events is typical of all the crack branchng that occurred.

Scanning electron micrographs of the branch region are shown in Fig. 7. Fig. 7a shows that one of the branches was initiated in the centre of the specimen. (This is the branch which formed from crack tip C.) The relatively smooth surface of this branch upon initiation indicates that an initiation it was a very low energy crack. Fig. 7b shows the other branch formed as a continuation of the original main crack. There is no discernable decrease in the surface roughness when branching occurred.

In specimens 5, 6, 7 and 8 (Table I) attempts at crack branching were observed. In an attempted branch sequence the crack front was observed to "twist" and tips A and B were formed. However no tip C formed and when tip B "overran" tip A, the crack continued on with one front, leaving only a "kink" in the fracture surface as evidence of the attempted branch.

5. A model for crack deceleration and crack branching

Before proposing a model to explain the occurrence of crack deceleration, and crack branching, Williams' [11] model of the crack tip region during constant crack speed environmental failure will be discussed.

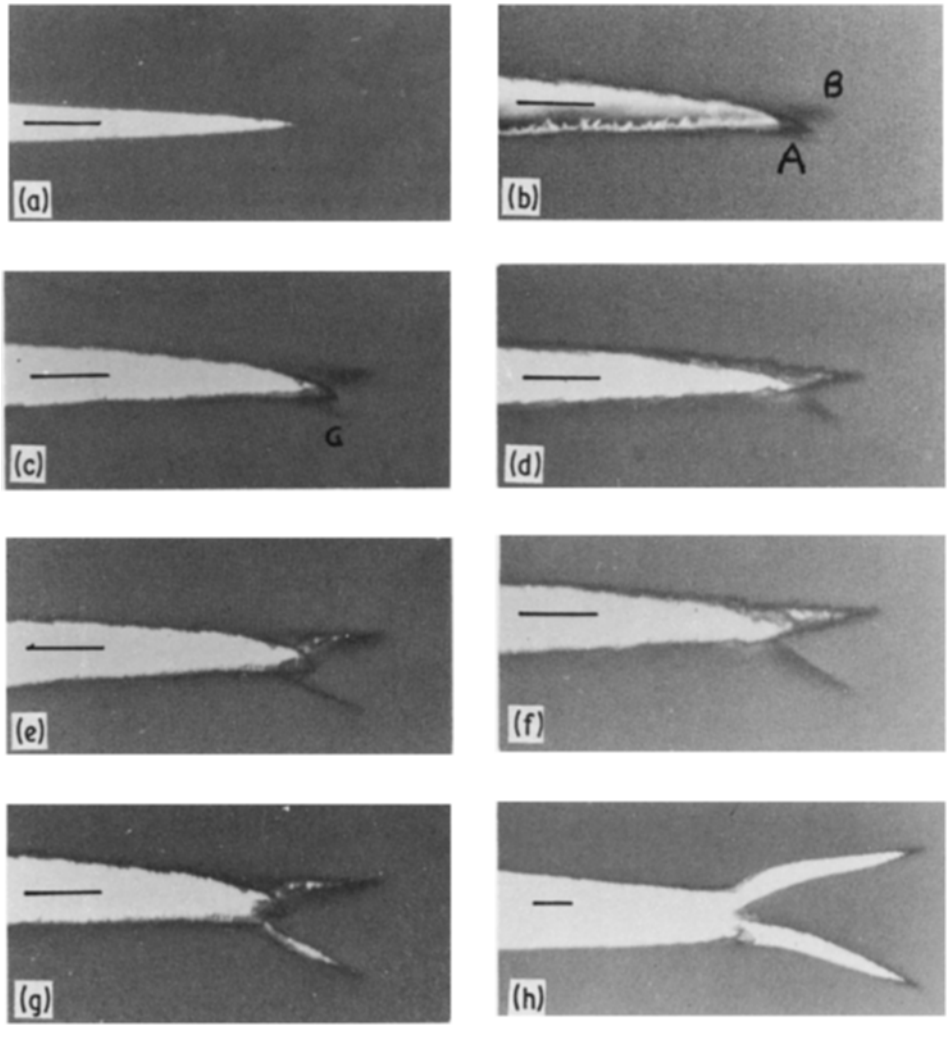

Figure 6 This series of photos shows the process of crack branching. The crack initially twisted producing Fronts A and B on the surfaces. A new branch, C, was then initiated in the specimen centre. Eventually B and C formed the two cracks. Scale = 10 mm. (a) Crack tip prior to branching, (b) Front of specimen, $t = 0$ min, (c) Front of specimen, $t = 35$ min, (d) Back of specimen, $t = 35$ min, (e) Front of specimen, $t = 70$ min, (f) Back of specimen, $t = 70$ min, (g) Front of specimen, $t = 120$ min and (h) Front of specimen, $t = 240$ min.

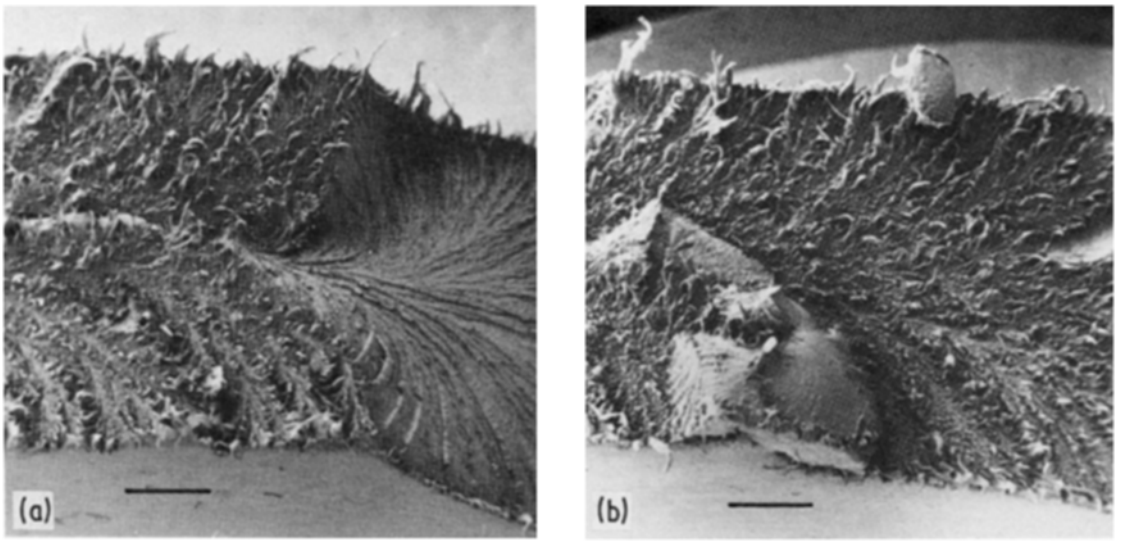

Figure 7 (a) Fracture surface showing centre initiated branch. Scale = 50 μm. (b) Fracture surface showing branch which formed as a continuation of the main branch.

Williams envisages that a two-stage craze zone exists at the crack tip as shown in Fig. 8. In this model r_p is the total craze length, r_o is the length of dry craze with load carrying capacity σ_c and $r_p - r_o$ is the length of wet craze with load carrying capacity reduced to $\alpha\sigma_c$ (where α is a constant such that $0 < \alpha \leqslant 1$) because of plasticization of the craze ligaments due to environments absorption. As the stress intensity increases during constant crack propagation, the proportion of the craze which is dry increases.

Williams assumes that failure occurs at a critical crack opening displacement, δ_c^*, which is a constant and that the craze stress, σ_c, and presumably the plasticization factor, α, are constant over the length of the craze. Fig. 2 shows a gradual increase in the length of the fibrils on the fracture surface. It may be assumed that the fibril length represents (half) the craze width when craze breakdown occurs. Thus it would appear that the crack opening displacement at which the craze breaks down is not a constant for this system. As the craze stress, σ_c, and the plasticization factor, α, may depend on fibril size, they also may not be constant for this particular system.

Despite objections to the details of Williams' model, it is convenient, and not unreasonable, to assume that the basic idea of a two-stage wet/dry craze ahead of the crack tip during constant crack propagation is correct. It has been established by Bandyopadhyay and Brown [12] that a craze does exist ahead of the crack tip during environmental stress cracking of the nature under discussion here. Williams' two-stage model provides an explanation for the existence of a constant crack speed region. There is something a single-stage, all-wet craze model cannot do. Accordingly, Williams' model will be used as the basis of the following description of a process by which it is thought crack deceleration and crack branching may occur.

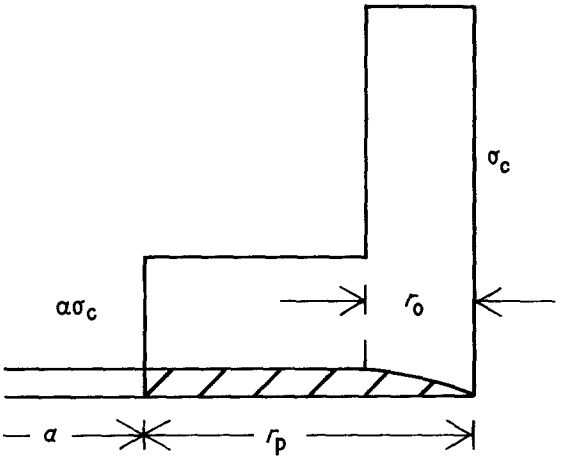

Figure 8 Schematic representation of the two stage craze zone present at the crack tip during propagation in region II (after Williams [11]).

Considering first the thinner specimens in which crack deceleration occurs, as the crack grows, the stress intensity factor at the crack tip increases; and the length of high stress dry craze must increase. A small region adjacent to the dry craze at (or near) the specimen edges will eventually become sufficiently stressed, for localized yielding rather than craze formation, to occur. Crack propagation occurs by the breakdown of the wet craze, so if the crack is to continue to propagate, the craze must grow above, below or around the yielded region. A non-planar fracture surface is likely to be produced and the rate of growth of the crack will be decreased. Eventually yielding will occur over most of the craze front, and craze and craze growth will stop completely. Failure by ductile tearing does not occur because the net stress on the uncracked portion of the specimen is much less than σ_y.

Evidence for this model comes from Fig. 3 where the existence of a non-planar fracture surface in the decelerating crack region is suggested by the irregular crack path on the surface of the specimen in that region. Further evidence comes from observations, made under polarized light, of microtomed sections taken perpendicular to both the fracture surface and the direction of crack growth (Fig. 9).

Fig. 9a shows a section typical of the beginning of the constant crack growth region. There is no evidence of yielding near the fracture surface. Fig. 9b is typical of the early stages of the decelerating crack region.

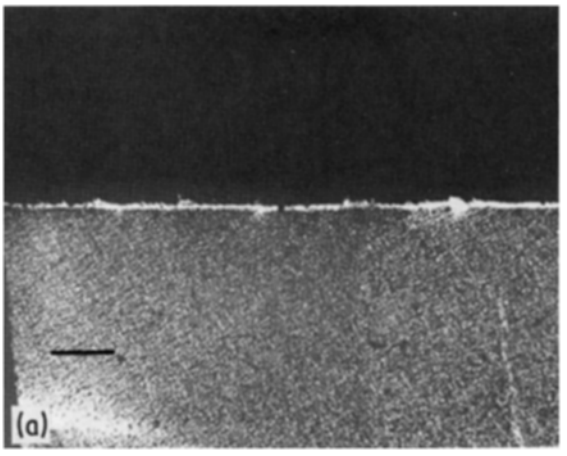

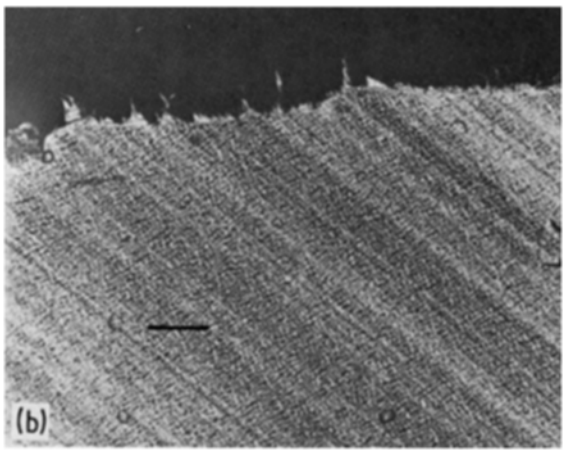

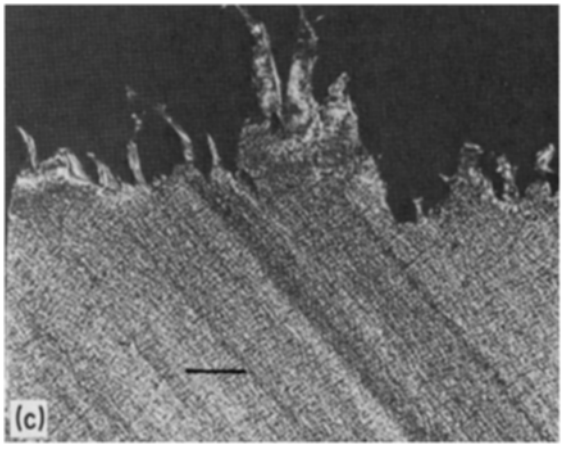

Figure 9 (a) Thin selection typical of the beginning of the constant speed crack growth region. The surface is planar and the fibrils are very small. Scale = 10 mm. (b) Thin selection typical of the early stage of the decelerating crack growth region. The surface has a step in it and the fibrils are longer. Below the left end of the fracture surface there is a region of different constrast indicating yielded material. (c) Thin section typical of the end of the decelerating crack growth region. The surface is very irregular and large fibrils are present. There are regions of different contrast, indicating yielding material, below the left end and the centre of the fracture surface.

Small yield zones are visible at the edges of the specimen. Fig. 9c represents the end of the decelerating crack region. Large yielded regions are evident just below the fracture surface.

Referring now to the 3.90 mm thick specimens in which crack branching occurs, it is envisaged that as the crack grows during constant crack propagation a similar process of localized yielding adjacent to the dry craze, at or near the specimen edges, begins to occur. However in these thick specimens the portion of the craze front which yields is not as large as for the thinner specimens. (The size of the yield zones is assumed to be dependent on stress, not on specimen thickness). The growth of the craze will not be hindered to the same extent and the portion of the craze which has grown above or below the yielded zone will continue to propagate at a nearly constant speed. This growth of the craze above or below the yield zones results in the twisting of the crack tip and the production of the two crack tips shown as crack tips A and B in Fig. 8. As these two crack tips grow, the material in the centre of the specimens is strained excessively, the internal crack shown as crack tip C in Fig. 8 is produced and crack branching occurs.

If an internal crack is not produced, as in type II specimens, then the crack does not branch. The crack decelerates slightly as the formation of yield zones continues. At a later stage, probably soon after the crack tip has "recovered" from the first attempt at branching, the crack front twists again; and if an internal crack is produced, then crack branching will occur. Why the twisting of the crack to produce tips A and B is not sufficient to result in crack branching is not known. From Fig. 7a showing the low energy fracture surface on initiation of the internal crack, it would appear that this crack forms as early as is possible. In type II specimens, for some reason, the internal crack is not able to nucleate the first time the crack tip twists.

6. Crack propagation subsequent to branching – results and discussion

The paths of the crack branch fronts subsequent to branching may be regarded as a special case of crack propagation under mixed Mode I and Mode II loading. Several criteria have been proposed for the crack path followed under this type of loading [13–21].

Cotterell and Rice [21] describe their criterion in terms of the requirement that pure Mode I conditions ($K_{II} = 0$) must exist at the advancing crack tip. They state that all the proposed criteria are consistent with this in that, for these other criteria if K_{II} is not zero at the crack tip, there will be an immediate abrupt change in the crack direction. Hence if a smooth crack path is produced, all the criteria imply K_{II} is zero as the crack extends.

Several workers have tried to determine the crack tip stress intensity factors of branched cracks [22–27]. Lo [25] provides the most complete K_I and K_{II} calculations; and he is in agreement with most other workers, his results will be summarized. Lo found that $K_{II} = 0$ when the included branch angle, 2θ, is 30° and $c/l = 6$ (see Fig. 10). His calculations also imply that as the branches grow (as c/l decreases), the angle at which $K_{II} = 0$ is likely to decrease. This agrees well with the observations made in these experiments that initially the included branch angle ranges from 30 to 40°, and that as the branches grow there is a tendency for them to curve in (that is for the angle between them to decrease).

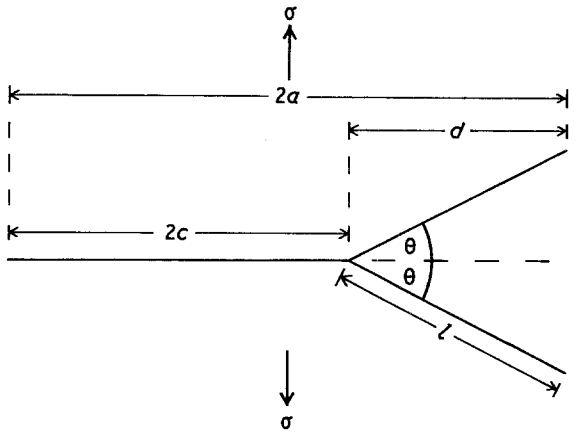

Figure 10 Geometry of symmetrically branched crack.

The velocities of the branch tips within each specimen were observed to be constant and equal. The constant branch velocities ranged from 2.0 to 2.5 mm h^{-1} for the various specimens.

This is less than the range of 2.6 to 2.9 mm h^{-1} observed for the crack tip before branching. Difficulties did exist in crack measurement after branching had occurred, the method employed involved measuring in a straight line from the point of branching to the branch tip. As the branches tended to curve in, the chord length rather than the actual crack length was measured. Thus the calculated branch velocities would have been slightly less than the actual branch velocities. However it is unlikely that the magnitude of the reduction in crack speed on branching can be explained in this manner, and it would appear that there is indeed a reduction in crack speed after branching. If indeed crack propagation subsequent to branching proceeds such that $K_{II} = 0$, the reason for the reduction in crack speed on branching is unclear. Possibly the equivalence of the various criteria for crack propagation under mixed mode loading, as proposed by Cotterell and Rice [21] is not exact. Thus at the branch tip there may be some small K_{II} component causing a distortion of the craze at the branch tip resulting in a reduction in the rate at which fluid can flow into the craze and thus a reduction in the speed of crack propagation.

In half the specimens (distributed evenly between type I and type II specimens) one of the crack branches was observed to rebranch. Again the included branch angle was observed to range from 30 to 40°, and there was a tendency for the branch paths (particularly the outer two paths) to curve in towards the horizontal. The branch speeds were again constant and equal.

7. Conclusions

At intermediate K values, a region where the crack speed is constant, independent of K, is observed in detergent cracking of LDPE. This region is terminated at high K by one of two processes: in thin specimens the crack arrests, and in thick specimens it branches. The mechanism of crack branching involves the crack front twisting and then the initiation of a new crack at the centre of the specimen. A model has been proposed to explain this mechanism and also the fact that crack arrest or branching occur at approximately the same K value. After branching the cracks continue to propagate at constant speed along paths where $K_{II} \approx 0$ and if the specimen is wide enough, can branch again.

References

1. M. E. R. SHANAHAN and J. SCHULTZ, *J. Polym. Sci., Polym. Phys. Ed.* **18** (1980) 1747.
2. S. BANDYOPADHYAY and H. R. BROWN, *Int. J. Fracture* **15** (1979) R175.
3. C. S. CARTER, *Corrosion* **15** (1969) 423.
4. *Idem, Met. Trans.* **1** (1970) 1551.
5. *Idem, Eng. Fracture Mech.* **3** (1971) 1.
6. M. O. SPEIDEL, in "The Theory of Stress Corrosion Cracking in Alloys", edited by J. C. Scully (NATO Scientific Affairs Division, Brussels, 1971).
7. A. M. SULLIVAN, *Eng. Fracture Mech.* **4** (1972) 65.
8. W. F. BROWN and J. E. SRAWLEY, ASTM STP 410 (American Society for Testing and Materials, 1966).
9. S. BANDYOPADHYAY and H. R. BROWN, *J. Polym. Sci., Polym. Phys. Ed.* **19** (1981) 749.
10. S. BANDYOPADHYAY, PhD thesis, Monash University, Australia (1979).
11. J. G. WILLIAMS, *Fortschr. Hochpolym. Forsch. (Adv. Polym. Sci.)* **27** (1978) 67.
12. S. BANDYOPADHYAY and H. R. BROWN, *Polym. Eng. Sci.* **20** (1980) 720.
13. F. ERDOGEN and G. C. SIH, *J. Bas. Eng. Trans. ASME* **85** (1963) 519.
14. J. G. WILLIAMS and P. D. EWING, *Int. J. Fracture Mech.* **8** (1972) 441.
15. P. D. EWING and J. G. WILLIAMS, *ibid.* **10** (1974) RCR 135.
16. I. FINNIE and A. SAITH, *ibid.* **9** (1973) RCR 484.
17. G. C. SIH, *Eng. Fracture Mech.* **5** (1973) 365.
18. *Idem, Int. J. Fracture* **10** (1974) 305.
19. R. V. GOLDSTEIN and R. L. SALGANIK, *ibid.* **10** (1974) 507.
20. M. C. HUSSAIN, S. L. PU and J. UNDERWOOD, ASTM STP 60 (American Society for Testing and Materials, 1974) 2.
21. B. COTTERELL and J. R. RICE, *Int. J. Fracture* **16** (1980) 155.
22. J. F. KALTHOFF, in "Dynamic Crack Propagation", edited by G. C. Sih (Leyden, Noordhoff, 1972) pp. 449–58.
23. B. A. BILBY, G. E. CARDEW and I. C. HOWARD, in "Fracture 1977", edited by D. M. R. Taplin, University of Waterloo Press, Waterloo, Canada, 1977) pp. 201–11.
24. H. KITTAGAWA, R. YUUKI and T. OHIRA, *Eng. Fracture Mech.* **7** (1975) 515.
25. K. K. LO, *J. Appl. Mech.* **45** (1978) 797.
26. P. S. THEOCARIS and N. IOAKIMIDIS, *Z. Angew. Math. Phys. (ZAMP)* **27** (1976) 801.
27. G. P. CHEREPANOV and V. D. KULIEV, *Int. J. Fracture* **11** (1975) 29.

Received 26 February
and accepted 25 April 1985